3.2 MODELED SENSITIVITY OF WINTERTIME PRECIPITATION TO CCN AND GCCN CONCENTRATIONS

Stephen M. Saleeby*
Colorado State University, Ft. Collins, Colorado
William R. Cotton
Colorado State University, Ft. Collins, Colorado

1. INTRODUCTION

It is widely known that higher CCN concentrations tend to decrease cloud droplet size, increase number concentration, and narrow the droplet spectrum (Warner 1967, Fitzgerald and Spyers-Duran 1973, Pruppacher and Klett 1997). However, Johnson (1982) and Feingold et al. (1999) showed that, in warm clouds, GCCN can act to accelerate and increase rain formation by reducing the colloidal stability of the cloud through broadening of the droplet distribution and enhanced collisional growth. From observations, Mather (1991) concluded that advertent or inadvertent seeding of clouds by large hygroscopic nuclei may enhance the precipitation process by accelerated "coalescence or coalescence-freezing mechanisms," and that ice formation may aid in this enhancement. Aerosol influences are not limited to warm cloud processes; it has been found that variability in aerosol concentrations can alter ice particle riming efficiencies (Hindman 1994; Borys 2000). More specifically, Borys (2000) found that increased sulfate-based aerosol concentrations suppress formation of larger cloud droplets and reduce riming of cloud droplets by ice hydrometeors. Pruppacher and Klett (1997) delineate 10μm to be the cloud droplet riming cut-off size below which riming efficiencies are near zero.

Walko et al. (1995) introduced the microphysics model of the Regional Atmospheric Modeling System at Colorado State University (RAMS) in the framework of one-moment prediction, and Meyers et al. (1997) extended this to two-moments of the distribution for rain, pristine ice, snow, aggregates, graupel, and hail. While the Meyers et al. (1997) version improved upon hydrometeor prognostic quantities, it still prognosed only mixing ratio of the cloud droplet distribution; as such, cloud droplet nucleation was treated very simplistically. If supersaturated conditions exist, the excess vapor is condensed from the vapor phase to the liquid droplet phase. The number concentration of newly formed droplets is diagnosed from the condensed water and a specified minimum droplet diameter of 2μm. Autoconversion of cloud droplets to rain is treated according to a quasi-bin approach (Feingold et. al 1988) using realistic collection kernels from Long (1974) and/or Hall (1980). This formulation is currently used in the prototype realtime version 4.3 of RAMS to produce daily forecasts.

Saleeby and Cotton (2004) extended the two-moment approach to the cloud droplet distribution via a parameterization for the formation of cloud droplets from activation of CCN and GCCN within a lifted parcel. The Lagrangian parcel model of Heymsfield and Sabin (1989), was utilized to determine the percent of user-specified CCN that would deliquesce, activate, and grow by condensation into cloud droplets for a given ambient temperature, vertical velocity, concentration of CCN, and median radius of the CCN distribution. The cloud droplet spectrum was further modified to behave as a bi-modal distribution with small cloud droplets (hereafter referred to as cloud1) from 2-40 μm in diameter and large cloud droplets (hereafter referred to as cloud2) from 40-80 μm in diameter. This bi-modal representation of the cloud droplet spectrum follows from observations of Hobbs et al. (1980) of a frequently occurring second peak in the droplet spectrum with diameters at the larger end approaching the size of drizzle droplets. Cloud2 acts as an intermediate size droplet category before droplets reach rain sizes; this slows the collection process to more realistic time scales. The parameterized activation of CCN (GCCN) and growth of their solution droplets results in direct formation of cloud1 (cloud2) droplets.

In this study we simulated a local, winter snowfall event over Colorado that occurred from 28-29 February 2004. This case represents a classic, northwesterly flow, high mountains snowfall event for Colorado and provides an excellent test case for examining the sensitivity of the new cloud droplet parameterization to the initial aerosol concentration and cold cloud processes as well as providing an objective comparison to the daily-run realtime RAMS model to assess any forecast improvement brought about by updating the cloud droplet parameterization.

2. MODEL DESCRIPTION

All simulations performed in this study were configured according to the specifications of the current RAMS prototype-realtime forecast model. This non-hydrostatic, compressible version of the model is configured on an Arakawa-C grid and sigma-z terrain-following coordinate system (Cotton et al. 2003). The model uses two-way nesting with a 3-grid arrangement for this particular application. The outer grid-1 covers the continental United States with a 48km grid spacing (100 x 72 pts), the nested grid-2 covers Colorado and the adjacent surrounding states with a 12km grid spacing (78 x 72 grid points), and lastly, a nested grid-3 encompasses most of Colorado with a 3km grid spacing (98 x 98 grid points). Within each grid there are 32 vertical levels with a minimum of 300m grid spacing; the

Corresponding author address: Stephen M. Saleeby, Colorado State Univ., Atmos. Sci. Dept., Fort Collins, CO 80523; e-mail: smsaleeb@atmos.colostate.edu

	Number of Predicted Moments		Number Concentration (cm-3)	
	Cloud1	Cloud2	CCN	GCCN
EXP01	1	0	n/a	n/a
EXP02	1	1	n/a	n/a
EXP03	2	1	100	n/a
EXP04	2	2	100	0.01000
EXP05	2	2	100	0.00001
EXP06	2	1	500	n/a
EXP07	2	2	500	0.01000
EXP08	2	2	500	0.00001
EXP09	2	1	1000	n/a
EXP10	2	2	1000	0.01000
EXP11	2	2	1000	0.00001

Table 1. List of variations in experiment initial conditions. All simulations were identical except for the variations shown above. The simulations used a CCN (GCCN) median radius of 0.04μm (3.0μm). Aerosol concentrations were initialized 3-D homogeneous.

model uses vertical grid stretching with a stretch ratio of 1.1 and a maximum vertical grid spacing of 750m.

For these simulations the model was initialized with 40km Eta forecast grids at 0000 UTC 28 February 2004 and was run for 39 hours. The base state simulations were run with two-moment microphysics prognosing hydrometeor mixing ratio and number concentration for rain, pristine ice, snow, aggregates, graupel, and hail. Two-moment prediction was implemented selectively for the two cloud droplet modes. Initial CCN and GCCN concentrations were user-specified and vary between simulations, as given in Table 1. In each simulation a number concentration for CCN and GCCN was specified at the start time, and the 3-D field was initialized homogeneously. Source and sink terms for the aerosols are active following initialization. The aerosol concentrations are represented by a polydisperse field on a lognormal distribution with a median radius for CCN (GCCN) of 0.04μm (3.0μm), respectively.

3. OBSERVED VS. MODELED PRECIPITATION

a. Model precipitation verification

The modeled time series of accumulated precipitation at Steamboat Springs, CO from all of the simulations as well as from the Steamboat Springs Ski Patrol Station Headquarters and the Rabbit Ears Pass SNOTEL station are shown in Figure 1. Each of the time series in this figure begin accumulation at the model start time of 0000 UTC 28 Feb and run through the final time at 1500 UTC 29 Feb. Despite the different model initializations of aerosols and cloud droplets, all of the simulations perform well in forecasting the accumulation of the liquid equivalent snowfall. The evident time lag between the simulations and the Steamboat Patrol Station gauge is likely due to a known multiple-hour reporting delay in the precipitation tipping bucket gauge (Dr. Randy Borys, personal communication). Despite this problem, the final accumulation magnitudes closely agree by 1500 UTC 28 Feb. Among the simulations, there exists a variability of 5mm (~20%) in total accumulated precipitation at Steamboat Springs. This variability emphasizes the need for realistic initialization of aerosol concentrations.

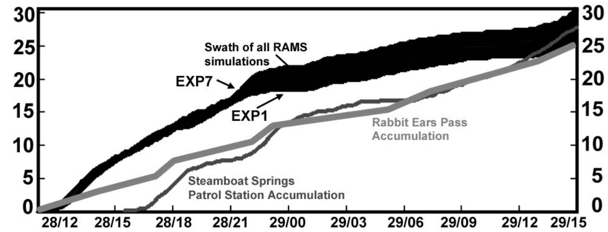

Figure 1. Time accumulated precipitation (mm) from RAMS simulations (dark, filled region; this encompasses the range of precipitation time series from all experiments), the Steamboat Springs ski resort precipitation gauge (dark gray line), and the nearby Rabbit Ears Pass SNOTEL site (light gray line).

Several SNOTEL sites were also chosen for comparison, and their locations are displayed on each panel in Figure 2. These stations are Bison Lake (BIS), Rabbit Ears Pass (RAB), Vail Pass (VAL), Joe Wright Reservoir (JOE), Bear Lake (BEA), and Lake Eldora (ELD). These sites are located along different mountain ranges and were chosen to assess the model variability among simulations and the model ability to forecast precipitation along varying topography. Table 2 displays the simulation-accumulated precipitation at the closest model grid point to each site for each sensitivity test as well as the observed values. The SNOTEL sites received only frozen precipitation, though they report the liquid equivalent amount. There is no single simulation that distinctly out-performs the others in forecasting the accumulations at the SNOTEL sites. For example, EXP 1 & 2 are closest to the observed values at BIS and JOE, while they comparatively produce the worst forecast at VAL and one of the poorest forecasts at BEA and ELD. A simple ranking formulation among simulations does suggest that use of the new droplet parameterization improves the precipitation prediction. The least (greatest) spread in the accumulation is 4.06mm (7.62mm). The range of precipitation extremes at the SNOTEL sites reveal a variation up to ~30% depending upon the model initialization of aerosol concentration. The total domain-averaged accumulated precipitation varies by a maximum range of ~1.0 mm (~10% variability) among the sensitivity experiments.

To put into perspective the variability in the total precipitation, we compared the modeled precipitation with the treated water usage for the city of Denver and for Colorado as a whole. On average, Colorado residents consume 865 million m^3 of treated

	BIS	RAB	STM	VAL	JOE	BEA	ELD
EXP01	29.46	25.40	25.91	24.89	36.32	22.86	15.24
EXP02	29.46	25.40	25.91	25.15	36.07	22.86	14.99
EXP03	36.07	23.62	27.94	19.81	30.23	18.80	13.21
EXP04	35.56	22.86	27.18	20.57	31.75	19.30	11.43
EXP05	35.56	24.13	28.19	18.03	31.50	20.32	13.46
EXP06	36.32	26.92	30.73	21.84	35.31	19.81	10.16
EXP07	35.56	25.91	29.72	21.84	32.51	22.35	12.19
EXP08	37.08	26.42	29.46	19.30	32.77	20.07	13.46
EXP09	35.31	24.89	27.18	20.57	31.24	22.86	13.97
EXP10	35.81	25.40	28.70	18.29	32.26	23.62	15.49
EXP11	35.56	24.38	26.67	19.56	34.80	21.84	13.46
Observed	27.94	27.94	28.19	20.32	35.56	15.24	12.70

Table 2. Accumulated precipitation (mm) from Steamboat Springs (STM), SNOTEL sites, and the respective values from each simulation. The SNOTEL sites are Bison Lake (BIS), Rabbit Ears Pass (RAB), Vail (VAL), Joe Wright Reservoir (JOE), Bear Lake (BEA), and Lake Eldora (ELD).

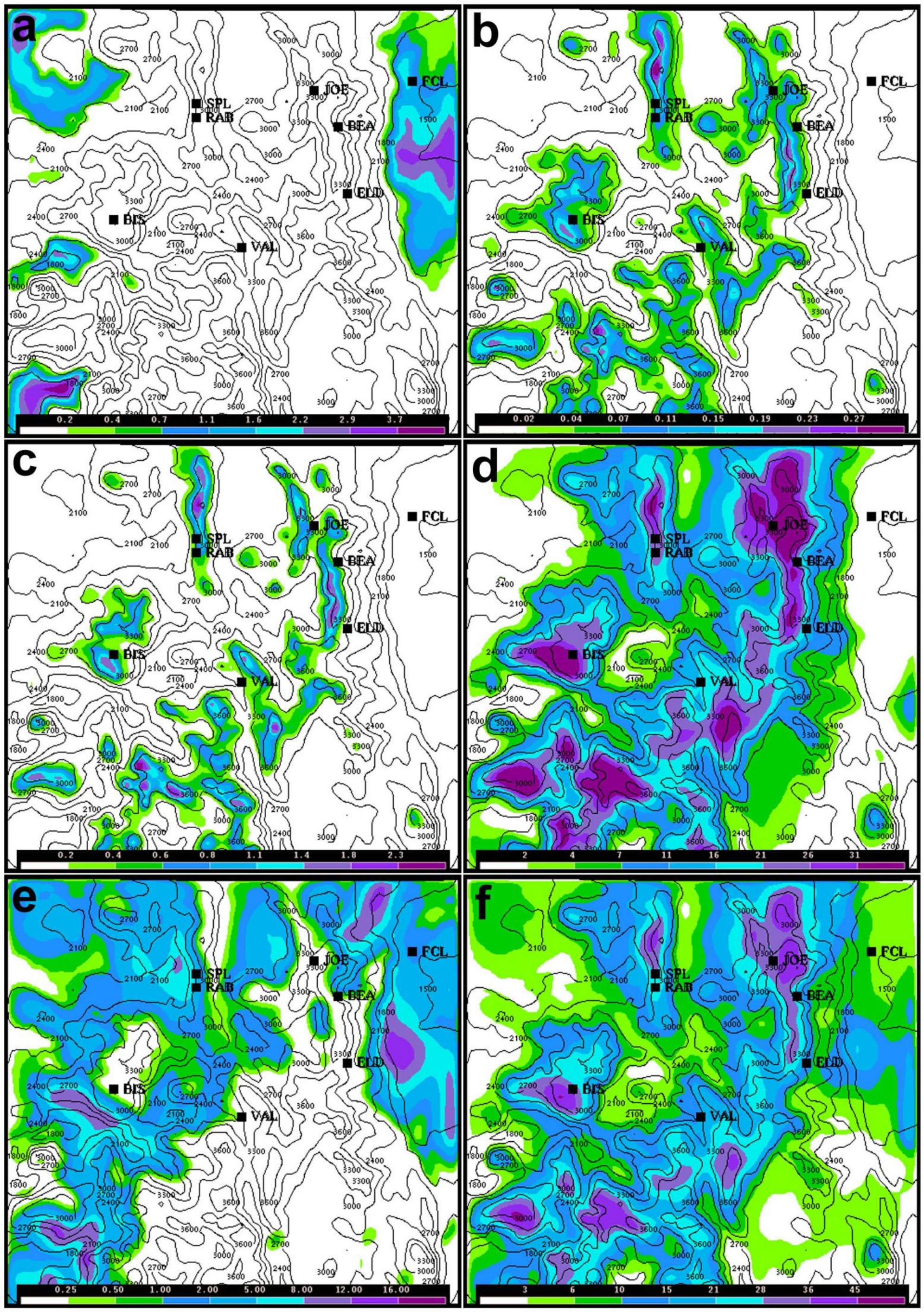

Figure 2. Total liquid equivalent accumulation (mm) of rain (a), pristine ice (b), snow (c), aggregates (d), graupel (e), and total precip (f) from 28/0000 - 29/1500 UTC from a single representative simulation. Topography (m) and SNOTEL locations are shown.

water per year, while Denver alone consumes 288 million m^3. Among the simulations, this single modeled snowstorm produced a minimum (maximum) amount of precipitation totaling 903 (989) million m^3 of surface precipitation accumulated over the whole of grid-3. This winter storm alone could provide more than a year's water supply if it could all be stored; furthermore, the maximum range of surface water for this one case amounts to nearly 86 million m^3. This variability of ~10% amounts to nearly one-third of Denver's yearly water consumption. Simulation EXP1 (EXP5) represented a polluted (non-polluted) type of environment, and it produced the minimum (maximum) precipitation.

b. Cloud droplet characteristics

Cloud1 droplet mixing ratio, number concentration, and mean diameter vary among simulations due to the variability in initial CCN and GCCN concentrations (Table 3). Aerosol concentrations directly determine the nucleation rate of cloud droplets in the model, and the variability in cloud droplet properties influences growth of the remaining hydrometeor types. The averaging of droplet properties was done for only those grid points with cloud water mixing ratio greater than the minimum threshold of 0.0001 g kg^{-1}. Generally, as the concentration of CCN was increased, the cloud1 mixing ratio and number concentration increased while the mean diameter decreased. When GCCN concentration was increased, the cloud1 mixing ratio and mean diameter decreased, and the number concentration increased.

While the values of cloud1 concentration are small and the mean diameters are rather large compared to typical observations (Borys 2000), these values are domain and time averaged over cloudy and nearly cloud-free areas, and thus, they do not give information on the instantaneous cloud field. Throughout the simulations, individual clouds contained regions with droplets concentrations up to 300 cm^{-3} and mean diameters < 10 μm (typical values measured at SPL while in-cloud). Furthermore, there was never substantial widespread “liquid cloudiness” since newly formed droplets did not remain in the liquid state for very long; the vapor growth and riming and collection processes efficiently moved the cloud water out of the cloud droplet categories. Also, much of the vapor available for droplet growth was consumed by pristine ice vapor growth (by the Bergeron-Findeisen process). Vertical cross-sections across the domain revealed an abundance of ice hydrometeors aloft, but relatively little liquid cloud water.

c. CCN impact on hydrometeor accumulation

Among experiments, accumulated rain was maximized for EXP3 in which GCCN were absent and the CCN concentration was minimized at 100 cm^{-3}. This relationship is consistent for both warm and cold cloud environments. A similarity exists between accumulated rain and aggregates, whereby, when GCCN are available, both hydrometeor categories experience an increase in accumulation as the number concentration of CCN is increased (Figure 3). In warm rain processes, higher CCN concentrations tend to suppress rain formation (Feingold et al. 1999); due to cold cloud processes occurring here, ice species effectively compete for cloud water through riming of sufficiently large cloud droplets. When CCN are increased in number, the resulting cloud1 droplets are smaller. This reduces vapor growth of all species as well as collection of cloud droplets since mean diameters of all hydrometeor types are reduced.

	Cloud1 LWC (g/kg)	Cloud1 Concentration (#/cm3)	Cloud1 Mean Diameter (μm)
EXP01	0.04368	n/a	n/a
EXP02	0.04353	n/a	n/a
EXP03	0.00943	0.6812	36.28
EXP04	0.00732	0.7733	34.30
EXP05	0.00919	0.6739	36.24
EXP06	0.01173	4.3450	29.79
EXP07	0.01110	4.6982	28.80
EXP08	0.01169	4.3490	29.80
EXP09	0.01132	11.1340	24.88
EXP10	0.00976	11.7520	24.16
EXP11	0.01086	10.9620	25.06

Table 3. Domain-averaged quantities for the cloud1 droplet mode. Only grid points with cloud1 LWC greater than 0.0001 g kg^{-1} were considered.

So why would aggregate mass increase if hydrometeor growth processes are reduced? Aggregates primarily grow by self-collection of pristine ice or snow or by collection of pristine ice or snow by existing aggregates. Following vapor deposition or collisional growth, aggregates are transferred to the graupel category if they acquire enough heat during these processes to develop a liquid layer. There is a competition between growth of aggregates and loss of aggregates from the development of a liquid surface layer. So, the combination of reduced vapor growth of aggregates and reduced collection of pristine ice and snow limits the formation of the aggregate liquid layer while still allowing slow growth of the aggregate category. Therefore, the increase in aggregate accumulation is not really an increase at all; it results, rather, from a reduced transfer of aggregates to graupel. Furthermore, the reduced conversion of aggregates to graupel, along with reduced vapor growth and collection of cloud droplets by graupel, causes graupel accumulation to decrease as CCN concentration increases.

Increased rain production at higher CCN concentrations is partially a result of competition among hydrometeor types. When the mean droplet size is reduced, droplet collection by ice species is significantly reduced, which leaves a higher reservoir of liquid droplet concentration and cloud water content. The droplet self-collection process is still effective for smaller droplets, such that self-collection still transfers liquid water to the rain category. There is a point of diminished returns, however, at which the droplets can be too small to efficiently self-collect; this is why we see the maximum cloud water transferred to rain for the mid-range number concentration of CCN (Table 4).

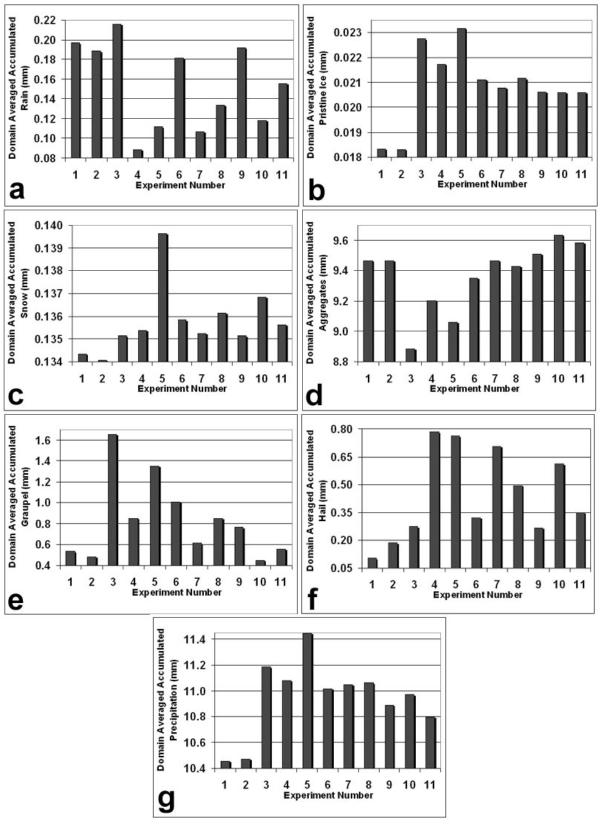

Figure 3. Charts of domain-averaged total surface accumulation (mm) of rain (a), pristine ice (b), snow (c), aggregates (d), graupel (e), hail (f) and total precipitation (g), for each of the sensitivity experiments.

The other main contributing factor to increased rainfall for greater CCN concentrations is the increased melting of graupel and hail and its transfer to rain. At higher CCN concentrations, graupel and hail have smaller mean diameters and smaller fall speeds. Over lower elevations, primarily the Colorado Front Range, these smaller hailstones more easily melt and spend more time below the freezing level. They subsequently reach the surface as rain rather than graupel or hail. Though not included here, surface plots of graupel, hail, and rain reveal co-located regions of increased rainfall and decreased graupel and hail.

d. GCCN impact on hydrometeor accumulation

For the experiments where GCCN were available, the rainfall was decreased when GCCN concentrations were increased (Figure 3). The introduction of GCCN reduced rainfall below that of the default realtime simulation. It is traditionally expected that in warm cloud processes an increased presence of GCCN (especially at high CCN concentrations) will lead to greater production of rainfall (Johnson 1982; Feingold et al. 1999). The presence of fewer, large droplets promotes rapid vapor growth to the critical size necessary for efficient collision-coalescence (~10μm), which leads to rain production (Pruppacher and Klett 1997). While these results tend to oppose the traditional

	Rain Collecting Cloud1	Graupel Collecting Cloud1	Rain Collecting Cloud2	Graupel Collecting Cloud2
EXP01	3.188E-06	6.931E-05	n/a	n/a
EXP02	5.034E-06	6.693E-05	1.787E-08	7.648E-08
EXP03	5.298E-06	1.517E-03	8.562E-09	2.300E-08
EXP04	4.887E-06	8.589E-04	6.849E-07	1.672E-04
EXP05	5.159E-06	1.480E-03	7.313E-09	6.102E-07
EXP06	7.161E-06	7.062E-04	2.381E-08	5.081E-08
EXP07	6.736E-06	5.644E-04	2.444E-07	3.819E-05
EXP08	7.287E-06	7.517E-04	2.451E-08	3.529E-07
EXP09	6.548E-06	4.268E-04	2.342E-08	5.385E-08
EXP10	6.096E-06	3.467E-04	1.431E-07	1.651E-05
EXP11	6.195E-06	3.882E-04	2.340E-08	3.069E-07

Table 4. Average domain-summed collected mass (kg) per model timestep for cloud droplets collected by rain and rimed by graupel. Rain and graupel were the two most dominant collector species.

thinking, we cannot assume that GCCN impacts are the same for cold cloud processes.

As the number concentration of GCCN is increased, there is greater competition with CCN for available excess vapor needed for cloud droplet formation. Since activation of CCN (GCCN) results in the formation of cloud1 (cloud2) droplets, an increase in GCCN produces an increase in cloud2 mixing ratio and number concentration and a decrease in cloud1 mixing ratio. Thus cloud1 droplets are relatively smaller in size while cloud2 droplets remain large enough to have high collision efficiencies. However, the impact of additional GCCN upon rainfall is diminished in this cold cloud environment since the ice hydrometeor classes compete with rain for the acquisition of cloud droplets. As previously mentioned, for a GCCN concentration increase, there is a decrease (increase) in the riming of cloud1 (cloud2) by graupel and collection of cloud1 (cloud2) by rain. The relative magnitude of the increase in collection of cloud2 by graupel is up to three orders of magnitude greater than that for rain. This effectively limits the cloud water that is available for rain production and results in less accumulated rainfall. Despite the dominance of graupel collection of cloud2 over that of rain, graupel accumulation also diminishes for an increase in GCCN concentration. This is due to reduced riming efficiency of cloud1, which is the dominant rimed species by an order of magnitude. Aggregates, however, are the only hydrometeor species that increase in surface accumulation when the concentration of GCCN is increased. This response is similar to that for increased CCN concentration, whereby, aggregates are more abundant due to reduced conversion to graupel. In terms of total accumulation, the GCCN influence is not consistent over the range of CCN concentrations. The greatest impact in this cold cloud environment occurs when CCN concentrations are lower.

4. CONCLUSIONS

The RAMS mesoscale model was utilized to perform a series of simulations whose purpose was to examine model sensitivity and variability to aerosol concentrations in a wintertime snow event that occurred during 28-29 February over the mountains of Colorado. From the preceding sections, we wish to emphasize the large range of model accumulated precipitation that was produced depending upon the cloud droplet parameterization and the initial aerosol concentration. Precipitation varied from 10% as a domain-wide average to 30% at an individual SNOTEL location. Comparisons made to the surface precipitation accumulation suggest that the default cloud droplet nucleation scheme used in the current realtime RAMS model tends to represent an extreme in droplet formation. These results favor improved model forecasting by representing more realistic droplet formation via the parameterization of CCN/GCCN activation.

Acknowledgments. We would like to thank Dr. Randy Borys for hosting the cloud microphysics class field project and for providing us with the realtime data from SPL. This research was supported by the National Science Foundation under grant ATM-0215367.

5. REFERENCES

Borys, R.D., D.H. Lowenthal, and D.L. Mitchell, 2000: The relationships among cloud microphysics, chemistry, and precipitation rate in cold mountain clouds. *Atmos. Environ*., **34**, 2593-2602.

Cotton, W. R., R. A. Pielke Sr., R. L. Walko, G. E. Liston, C. J. Tremback, H. Jiang, R. L. McAnelly, J. Y. Harrington, M. E. Nicholls, G. G. Carrio, and J. P. McFadden, 2003: RAMS 2001: Current status and future directions. *Meteorol. Atmos. Phys*., **82**, 5-29.

Feingold, G., S. Tzivion, and Z. Levin, 1988: Evolution of raindrop spectra. Part I: Solution to the stochastic collection/breakup equation using the method of moments. *J. Atmos. Sci*., **45**, 3387-3399.

_________, W.R. Cotton, S. Kreidenweis, and J. Davis, 1999: The impact of giant cloud condensation nuclei on drizzle formation in stratocumulus: implications for cloud radiative properties. *J. Atmos. Sci*., **56**, 4100-4117.

Fitzgerald, J.W. and P.A. Spyers-Duran, 1973: Changes in cloud nucleus concentration and cloud droplet size distribution associated with pollution from St. Louis. *J. Appl. Meteor*., **12**, 511-516.

Hall, W., 1980: A detailed microphysical model within a two-dimensional dynamic framework: Model description and preliminary results. *J. Atmos. Sci*., **37**, 2486-2507.

Hindman, E.E., M.A. Campbell, and R.D. Borys, 1994: A ten-winter record of cloud-droplet physical and chemical properties at a mountiantop site in Colorado. *J. Appl. Meteor*., **33**, 797-807.

Heymsfield, A. J., and R. M. Sabin, 1989: Cirrus crystal nucleation by homogeneous freezing of solution droplets. *J. Atmos. Sci*., **46**, 2252-2264.

Hobbs, P.V., M.K. Politovich, and L.F. Radke, 1980: The Structures of Summer Convective Clouds in Eastern Montana. I: Natural Clouds. *J.Appl. Meteor*., **19**, 645–663.

Johnson, D. B., 1982: The role of giant and ultragiant aerosol particles in warm rain initiation. *J. Atmos. Sci*., **39**, 448-460.

Kain, J.S., and J.M. Fritsch, 1993: Convective parameterization for mesoscale models: The Kain-Fritsch scheme. The Representation of Cumulus Convection in Numerical Models, *Meteor. Monogr.*, **46**, Amer. Meteor. Soc., 165-170.

Long, A., 1974: Solutions to the droplet collection equation for polynomial kernels. *J. Atmos. Sci*., **31**, 1040-1052.

Mather, G.K., 1991: Coalescence enhancement in large multicell storms caused by the emissions from a Kraft paper mill. *J. Appl. Meteor*., **30**, 1134-1146.

Meyers, M.P., R.L. Walko, J.Y. Harrington, and W.R. Cotton, 1997: New RAMS cloud microphysics parameterization. Part II. The two-moment scheme. *Atmos. Res*. **45**, 3-39.

Pruppacher, H., and J. Klett: 1997. Microphysics of Clouds and Precipitation. Second Revised Edition. Volume 18. Kluwer Academic Publishers. Dordrecht/Boston/London. Printed in The Netherlands.

Saleeby, S.M., and W.R. Cotton, 2004: A large droplet mode and prognostic number concentration of cloud droplets in the Colorado State University Regional Atmospheric Modeling System (RAMS). Part I: Module descriptions and supercell test simulations. *J. Appl. Meteor*., **43**, 182-195.

Walko, R.L., W.R. Cotton, M.P. Meyers, and J.Y. Harrington, 1995: New RAMS cloud microphysics parameterization: Part I. The single-moment scheme. *Atmos. Res*., **38**, 29-62.

Warner, J. and S. Twomey, 1967: The Production of Cloud Nuclei by Cane Fires and the Effect on Cloud Droplet Concentration. *J. Atmos. Sci*., **24**, 704–706.